

# Molecular Language Model as Multi-task Generator

Yin Fang<sup>1 2 3</sup> Ningyu Zhang<sup>1 4 2</sup> Zhuo Chen<sup>1 2</sup> Xiaohui Fan<sup>3 5</sup> Huajun Chen<sup>1 2</sup>

## Abstract

Molecule generation with desired properties has grown immensely in popularity by disruptively changing the way scientists design molecular structures and providing support for chemical and materials design. However, despite the promising outcome, previous machine learning-based deep generative models suffer from a reliance on complex, task-specific fine-tuning, limited dimensional latent spaces, or the quality of expert rules. In this work, we propose MOLGEN, a pre-trained molecular language model that effectively learns and shares knowledge across multiple generation tasks and domains. Specifically, we pre-train MOLGEN with the chemical language SELFIES on more than 100 million unlabelled molecules. We further propose multi-task molecular prefix tuning across several molecular generation tasks and different molecular domains (synthetic & natural products) with a self-feedback mechanism. Extensive experiments show that MOLGEN can obtain superior performances on well-known molecular generation benchmark datasets. The further analysis illustrates that MOLGEN can accurately capture the distribution of molecules, implicitly learn their structural characteristics, and efficiently explore the chemical space with the guidance of multi-task molecular prefix tuning<sup>1</sup>.

<sup>1</sup>College of Computer Science and Technology, Zhejiang University <sup>2</sup>Alibaba-Zhejiang University Joint Research Institute of Frontier Technologies <sup>3</sup>Pharmaceutical Informatics Institute, College of Pharmaceutical Sciences, Zhejiang University <sup>4</sup>School of Software Technology, Zhejiang University <sup>5</sup>Future Health Laboratory, Innovation Center of Yangtze River Delta, Zhejiang University. Correspondence to: Ningyu Zhang <zhangningyu@zju.edu.cn>, Huajun Chen <huajunsir@zju.edu.cn>.

*Work in progress.*

<sup>1</sup>Codes, datasets, and the pre-trained model will be available in <https://github.com/zjunlp/MolGen>.

## 1. Introduction

Molecular generation – synthesizing and designing novel molecules with desirable properties<sup>2</sup> – holds an important place in chemical science, with numerous applications in drug discovery (Wang et al., 2022a). The task of molecular generation is rather challenging, whereas the chemical space of molecules, being both discrete and vast with an estimated size of  $10^{33}$ , renders exhaustive searches infeasible (Polishchuk et al., 2013). Early, deep generative models (Jin et al., 2020; Zang & Wang, 2020; Luo et al., 2021; Shi et al., 2020b) have been proposed as one of the most promising tools for exploring the broader synthetically accessible chemical space. Their ability to automatically generate chemically valid and similar molecular structures has proven invaluable for tasks such as the inverse design of functional compounds (Flam-Shepherd et al., 2022).

Current deep generative models typically involve initial training of an unconditional generative model through a large dataset of existing molecules, followed by the employment of additional reward functions (Cao & Kipf, 2018; Popova et al., 2018; You et al., 2018; Popova et al., 2019; Shi et al., 2020b; Zang & Wang, 2020) or property predictors (Simonovsky & Komodakis, 2018; Jin et al., 2019; Gómez-Bombarelli et al., 2018; Liu et al., 2018) to guide the synthesis of new molecules with desired properties. Despite their widespread use, the performance of these approaches is limited by their reliance on heavy task-specific fine-tuning (Xie et al., 2021), fixed-dimensional latent generation space (Wang et al., 2022b), and expert-provided generation rules (Sun et al., 2022), which impede efficient exploration of the broader chemical space.

Recent advancements in language models have demonstrated their potential for understanding complex molecular distributions (Flam-Shepherd et al., 2022). Researchers have begun integrating SMILES (Weininger, 1988), a linear string notation for describing molecular structures, with pre-trained language models to gain a more comprehensive understanding of the underlying molecular structures and their representations (Irwin et al., 2022). However, the brittleness of SMILES may lead to a high proportion of generated SMILES strings being chemically invalid. These strings can

<sup>2</sup>This paper focuses on generating 2D molecules based on given molecules, also known as molecular optimization.

either be syntactically incorrect (e.g., not corresponding to molecular graphs) or violate fundamental chemical principles (e.g., exceeding the maximum number of inter-atomic valence bonds). Another defect is that current language model-based approaches rely on task-specific fine-tuning with different optimization objectives, making each progress incompatible and hindering knowledge sharing among multiple downstream tasks. Besides, almost all previous studies have primarily focused on one single domain of synthetic molecules, neglecting natural products. Notably, natural products, characterized by enormous scaffold diversity and structural complexity, exhibit a distinct distribution compared to synthetic molecules and confer additional opportunities and challenges for numerous molecular generation applications such as drug discovery (Atanasov et al., 2021).

In this paper, we propose MOLGEN, a novel pre-trained molecular language model for molecular generation. Specifically, to effectively explore the chemical universe, **Firstly**, we pre-train a molecular language model based on the chemical language SELFIES (Krenn et al., 2020), where each combination of symbols in its alphabet maps to a chemically valid graph. By combining bidirectional and auto-regressive Transformers (Vaswani et al., 2017), the pre-trained molecular language model can learn intrinsic structural regularities by mapping corrupted SELFIES to their original forms. **Then**, to break down the boundaries between diverse molecular tasks and domains (synthetic & natural products), we introduce Multi-task molecular Prefix Tuning (MPT). It allows the model to acquire general features that can be transferred to various domains, thus simplifying the process of adapting to new tasks. Moreover, by incorporating a simple self-feedback paradigm that assigns probabilities to candidate molecules based on their property scores, MOLGEN is incentivized to generate molecules with desired properties.

We conduct comprehensive experiments on both synthetic and natural product molecular datasets. The considerable performance gains on molecular generation benchmarks demonstrate the capability of MOLGEN to generate chemically valid molecules and effectively navigate the chemical space. We further investigate MOLGEN’s understanding of molecular distributions, recognition of crucial substructures, and the effect of MPT. Our findings confirm that MOLGEN preserves generation diversity while mastering the distribution and structural characteristics of molecules. Additionally, MPT improves the performance on various tasks, owing to its ability of knowledge sharing.

## 2. Related Work

**Molecular generation.** The past decade has seen significant progress in molecule generation, particularly in deep generative models (Gómez-Bombarelli et al., 2018). Prior works typically formulate this task as a sequence genera-

tion problem. Specifically, (Kusner et al., 2017; Gómez-Bombarelli et al., 2018; Segler et al., 2018; Kwon et al., 2021) start by generating SMILES strings due to the abundance of sequence modeling tools such as recurrent neural networks, dilated convolutions, and attention mechanisms. Additionally, as molecules can be naturally viewed as two-dimensional graphs, various molecular graph-based generative methods have emerged (Ma et al., 2018; Simonovsky & Komodakis, 2018; Jin et al., 2020; Zang & Wang, 2020; Luo et al., 2021). Based on these two forms of representation, existing approaches can be categorized into four venues.

**Bayesian Optimization (BO)** (Gómez-Bombarelli et al., 2018; Jin et al., 2018; Winter et al., 2019) learns a continuous latent space of molecules and optimizes the target properties by navigating through this space. However, BO often requires a long evaluation time to optimize the objective function (Du et al., 2022). **Reinforcement Learning (RL)**-based approaches aim to train an agent to select actions, such as adding substructures, in an explicit chemical space to optimize properties (Cao & Kipf, 2018; Popova et al., 2018; You et al., 2018; Popova et al., 2019; Shi et al., 2020b; Zang & Wang, 2020), but these methods are often difficult to optimize due to high variance (Xie et al., 2021). **Variational Auto-Encoder (VAE)** can be another solution (Simonovsky & Komodakis, 2018; Jin et al., 2019; Gómez-Bombarelli et al., 2018; Liu et al., 2018), but their performance is highly dependent on the quality of the fixed-dimensional latent space. Lastly, **Genetic Algorithms (GA)** (Jensen, 2019; Ahn et al., 2020; Nigam et al., 2020) use predefined mutation and crossover rules from reference compound libraries or domain expertise to generate molecules. While flexible, it can be challenging to acquire the necessary prior knowledge and rules, limiting the search process’s efficiency.

**Pre-trained language models.** Pre-trained language models (PLMs) have waved the community as fundamental infrastructure (Kenton & Toutanova, 2019; Lewis et al., 2020; Brown et al., 2020). Intuitively, PLMs are a promising solution for molecular generation, and several pioneers have started to leverage SMILES-based language models with promising performance (Bagal et al., 2021; Irwin et al., 2022; Flam-Shepherd et al., 2022; Ross et al., 2022; Chilingaryan et al., 2022; Pan, 2023). To date, **Chemformer** (Irwin et al., 2022) is the only publicly available PLM that can address molecular generation tasks. Note that similar to human language, molecular language also has syntax, and just as the syntax of natural languages imposes a grammatical structure that allows words to relate to each other in specific ways, biological symbols also combine in specific structural manners. However, SMILES, as a traditional molecular language, contains complex and restrictive grammars, which results in most sequences over the appropriate character set not belonging to well-defined molecules. Com-

pared with **Chemformer** and other previous approaches, MOLGEN has two main differences: (1) We pre-train the language model with SELFIES, a chemical language representation of molecules that is 100% robust to both syntactic and semantic issues. (2) We formulate downstream tasks with multi-task molecular prefix tuning to share knowledge across tasks and domains (synthetic & natural products).

### 3. Methodology

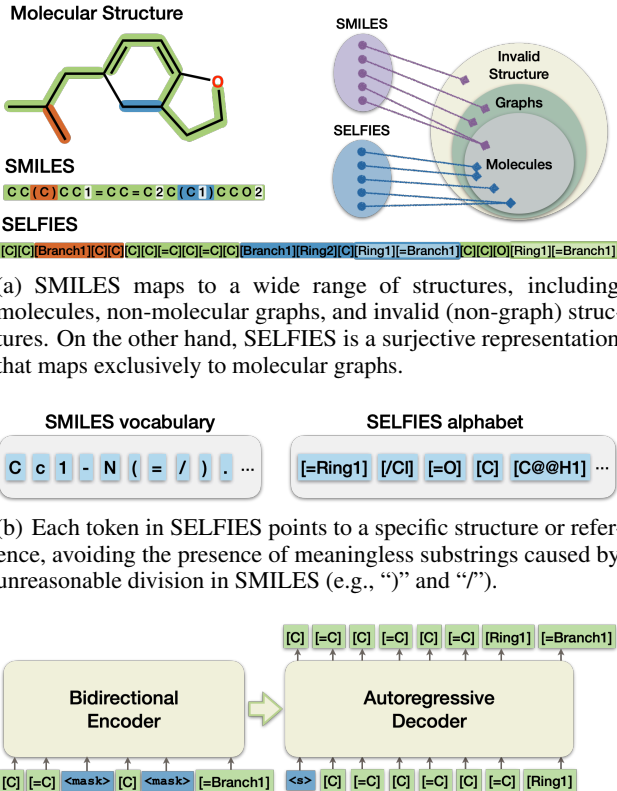
As shown in Figure 2, we illustrate the general framework of MOLGEN, which is based on pre-training a molecular language model using SELFIES. We introduce the technical details of problem formulation (§3.1), generative molecular pre-training (§3.2), and multi-task molecular prefix tuning (§3.3) in the following sections.

#### 3.1. Problem Formulation and Background

We focus on three standard molecular generation setting in this paper. Concretely, define  $\mathcal{M} = \{M_i\}_{i=1}^n$  as a set of molecules,  $\mathcal{A}(M) : \mathcal{M} \rightarrow \mathbb{R}$  as a property score function, and  $\text{sim}(M, M') \in [0, 1]$  as a similarity function measures the similarity between the molecules  $M$  and  $M'$ . Then we formulate the molecular generation tasks as follows:

- *Distribution learning*: learning a generative model  $p_\theta(\cdot)$  from  $\mathcal{M}$ , such that the model can sample a valid molecule  $M$  with a high probability  $p_\theta(M)$ .
- *Targeted molecule discovery*: learning a targeted molecule discovery model  $p_\theta(\cdot)$  to maximize the expected property score  $\mathbb{E}_{M \sim p_\theta}[\mathcal{A}(M)]$ .
- *Constrained molecular property optimization*: learning a constrained optimization model  $p_\theta(\cdot|M)$ , to maximize  $\mathbb{E}_{M' \sim p_\theta}[\mathcal{A}(M')]$  while ensuring that  $\text{sim}(M, M') > \delta$  is satisfied. Here  $M'$  is the optimized molecule based on  $M$ , and  $\delta$  is a similarity threshold.

To address the task of molecular generation with PLMs, the current study (Irwin et al., 2022) follows BART (Lewis et al., 2020), a large pre-trained Seq2seq language model standard in the literature, to corrupt SMILES and then optimizing a reconstruction loss for pre-training. Specifically, the pre-training includes random sampling tokens within the original SMILES string  $S = \{s_1, \dots, s_j, \dots, s_l\}$  and replacing them with a special token [MASK], encoding the corrupted SMILES using a bidirectional model, and then calculating the likelihood of  $S$  with a left-to-right autoregressive decoder. Formally, we have the cross-entropy between the decoder’s output, and the original input constitutes the



(c) Reconstruct the SELFIES from the corrupted one by optimizing the negative log-likelihood object.

Figure 1. Generative molecular pre-training with SELFIES.

reconstruction loss as:

$$\mathcal{L}_{\text{ce}}(S) = - \sum_{j=1}^l \sum_s p_{\text{true}}(s|S, S_{<j}) \log p_\theta(s|S, S_{<j}; \theta),$$

where  $S_{<j}$  denotes the partial original sequence  $\{s_0, \dots, s_{j-1}\}$  and  $s_0$  is a pre-defined start token  $\langle s \rangle$ .  $p_{\text{true}}$  is a one-hot distribution under the standard maximum likelihood estimation:

$$p_{\text{true}}(s|S, S_{<j}) = \begin{cases} 1, & s = s_j \\ 0, & s \neq s_j \end{cases}.$$

#### 3.2. Generative Molecular Pre-training with SELFIES

SMILES and SELFIES are two molecular languages that map a string of tokens to a molecular graph. As illustrated in Fig 1(a), in SMILES, molecules are represented as chains of atoms (main string in green) with branches (red) defined within parentheses and ring closures (blue) indicated by two matching numbers. Although SMILES has been a workhorse in cheminformatics for the past few decades, it is

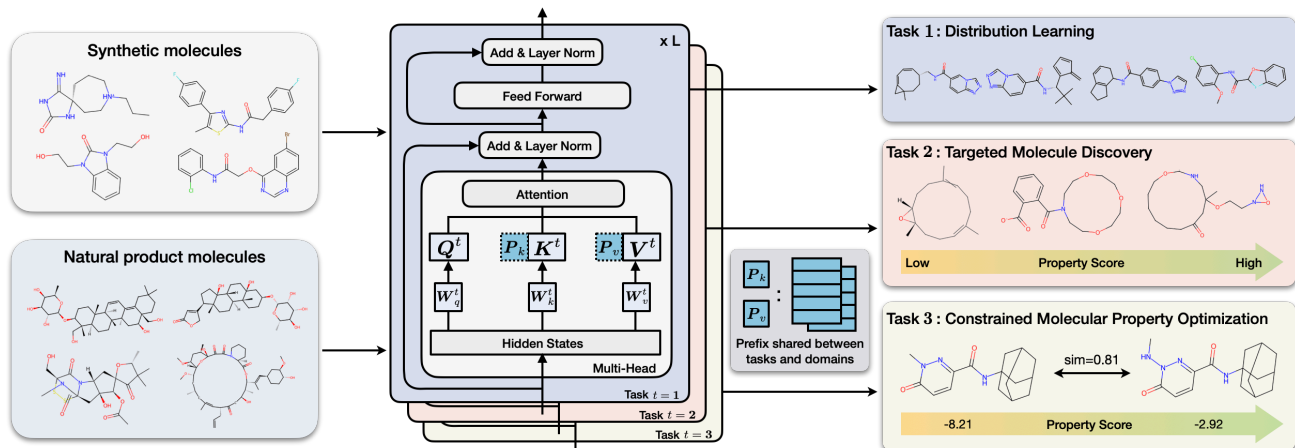


Figure 2. Multi-task molecular Prefix Tuning (MPT), which can share knowledge across tasks and domains (synthetic & natural products).

inherently fragile as there is no mechanism to guarantee that molecular strings can be valid regarding syntax and physical principles. This means that SMILES is a surjective representation from strings to structures that include molecular graphs but also non-molecular (semantically invalid) graphs and other structures which cannot be interpreted as graphs (syntactically invalid) (Krenn et al., 2020).

This weakness has been addressed by a 100% robust molecular language SELFIES, which is a surjective mapping from strings to molecular graphs. It means that SELFIES cannot produce invalid molecules since every combination of symbols in the SELFIES alphabet maps to a chemically valid graph (Krenn et al., 2022). Both rings and branches in SELFIES are defined at a single location, eliminating syntactic invalidity caused by unbalanced parentheses or ring identifiers. Special symbols start a branch ([Branch1]) or ring ([Ring1]), and the subsequent token in the string defines the length of the branch or ring according to its specific derivation rules (Krenn et al., 2022).

To pre-train the molecular language model, we collect more than 100 million unlabelled molecules as our pre-training corpus by randomly selecting from the publicly accessible ZINC-15 dataset (Sterling & Irwin, 2015) (the same pre-training corpus of Chemformer (Irwin et al., 2022) for a fair comparison). The selection process strictly follows the constraints outlined in Irwin et al. (2022), ensuring that the molecules are reactive, available for purchase, have a molecular weight of  $\leq 500$  Daltons, and a LogP (octanol-water partition coefficient) of  $\leq 5$ . The molecules are then converted to SELFIES strings and segmented into tokens. The use of SELFIES eliminates the need for training a specific tokenizer to identify frequently occurring substring patterns. Instead, we construct an alphabet from the dataset of SELFIES strings, as depicted in Fig 1(b), effectively avoiding

the generation of meaningless tokens caused by imprecise tokenization. We then conduct token masking on the input SELFIES strings  $S^* = \{s_1^*, \dots, s_l^*\}$  and train a Seq2Seq model to reconstruct the original SELFIES by optimizing the negative log-likelihood  $\mathcal{L}_{ce}(S^*)$ , as shown in Fig 1(c).

### 3.3. Multi-task Molecular Prefix Tuning

In current task-specific fine-tuning strategies to leverage PLMs, the inputs for molecular generation tasks contain diverse and structured knowledge from various molecular domains, making it difficult to effectively learn shared parameters. To address this challenge, we propose to break down the boundaries between tasks and domains through Multi-task molecular Prefix Tuning (MPT). Specifically, we prepend  $l$  tunable prefix vectors, shared between all generation tasks across domains, to the keys and values of the multi-head attention at every layer. Let  $\mathcal{T} = \{t\}_{t=1}^n$  denote the task type on one molecular domain; the attention score output on each head for the task  $t$  can be formulated as:

$$\text{head}^t = \text{Attn}(x^t W_q^t, [P_k, X^t W_k^t], [P_v, X^t W_v^t]),$$

where the sequence of  $m$  vectors  $X^t \in \mathbb{R}^{m \times d}$  denotes the input to a Transformer layer,  $x \in \mathbb{R}^d$  is a query vector, and  $W_q, W_k, W_v \in \mathbb{R}^{d \times d_h}$  are project matrices that map inputs to queries, keys, and values. Two sets of  $l$  prefix vectors  $P_k, P_v \in \mathbb{R}^{l \times d}$ , are concatenated with the original attention key and value in order to capture shared knowledge across all generation tasks. From an alternative view, the



computation of head<sup>t</sup> can be equivalent becomes:

$$\begin{aligned}
 \text{head}^t &= \text{softmax} \left( \mathbf{x}^t \mathbf{W}_q^t [\mathbf{P}_k, \mathbf{X}^t \mathbf{W}_k^t]^\top \right) \begin{bmatrix} \mathbf{P}_v \\ \mathbf{X}^t \mathbf{W}_v^t \end{bmatrix} \\
 &= \text{softmax} \left( \mathbf{x}^t \mathbf{W}_q^t \begin{bmatrix} \mathbf{P}_k^\top \\ (\mathbf{W}_k^t)^\top (\mathbf{X}^t)^\top \end{bmatrix} \right) \begin{bmatrix} \mathbf{P}_v \\ \mathbf{X}^t \mathbf{W}_v^t \end{bmatrix} \\
 &= \lambda(\mathbf{x}) \text{softmax} \left( \mathbf{x}^t \mathbf{W}_q^t \mathbf{P}_k^\top \right) \mathbf{P}_v \\
 &\quad + (1 - \lambda(\mathbf{x})) \text{softmax} \left( \mathbf{x}^t \mathbf{W}_q^t (\mathbf{W}_k^t)^\top (\mathbf{X}^t)^\top \right) \mathbf{X}^t \mathbf{W}_v^t \\
 &= \lambda(\mathbf{x}) \underbrace{\text{Attn}(\mathbf{x}^t \mathbf{W}_q^t, \mathbf{P}_k, \mathbf{P}_v)}_{\text{attention of prefix shared between tasks}} \\
 &\quad + (1 - \lambda(\mathbf{x})) \underbrace{\text{Attn}(\mathbf{x}^t \mathbf{W}_q^t, \mathbf{X}^t \mathbf{W}_k^t, \mathbf{X}^t \mathbf{W}_v^t)}_{\text{original attention}},
 \end{aligned}$$

where  $\lambda(\mathbf{x})$  is a scalar whose two terms in the denominator represent the sum of prefixes attention weights and original sequence normalized attention weights, respectively:

$$\lambda(\mathbf{x}) = \frac{\sum_i \exp(\mathbf{x}^t \mathbf{W}_q^t \mathbf{P}_k^\top)_i}{\sum_i \exp(\mathbf{x}^t \mathbf{W}_q^t \mathbf{P}_k^\top)_i + \sum_j \exp(\mathbf{x}^t \mathbf{W}_q^t (\mathbf{W}_k^t)^\top (\mathbf{X}^t)^\top)_j}.$$

This modification to the original head attention through linear interpolation with shared prefixes enables knowledge sharing across multiple domains and tasks.

#### Coordinating generation candidate with self-feedback.

For molecular generation tasks such as targeted molecule discovery and constrained optimization, the target is to assign higher probabilities to molecules with desired properties during inference, which is non-trivial for vanilla autoregressive generation. To this end, we introduce a simple mechanism dubbed coordinating generation candidate with self-feedback inspired by fine-tuning with human feedback (Ouyang et al., 2022) to bridge this gap. We hypothesize that the probability of a generated candidate molecule should be well-correlated with its property score as evaluated by an automatic metric  $\mathcal{A}$ . That is, for non-reference candidate SELFIES  $\hat{S}^*$ , we assume that:

$$\begin{aligned}
 p_{\text{true}}(S_i^* | S^*) &> p_{\text{true}}(S_j^* | S^*), \quad \forall S_i^*, S_j^* \in \hat{S}^* \\
 \mathcal{A}(S_i^*) &> \mathcal{A}(S_j^*),
 \end{aligned}$$

where  $S_i^*$  and  $S_j^*$  are two different candidate SELFIES, and  $S^* = \{s_1^*, \dots, s_l^*\}$  is the reference SELFIES. We utilize our model to generate various candidate SELFIES  $\hat{S}^*$ , each with distinct property scores, and then encourage the model to assign higher estimated probabilities to better candidates by MPT with a rank loss (Liu et al., 2022):

$$\mathcal{L}_{\text{rank}}(S^*) = \sum_i \sum_{j>i} \max(0, f(S_j^*) - f(S_i^*) + \lambda_{ij}),$$

where  $\mathcal{A}(S_i^*) > \mathcal{A}(S_j^*), \forall i, j, i < j$ .  $\lambda_{ij} = (j - i) * \lambda$  is the margin multiplied by the difference in rank between the candidates, and  $f(S_i^*)$  is the estimated log-probability:

$$f(S^*) = \sum_{t=1}^l \log p_\theta(s_t^* | S^*, S_{<t}^*; \theta).$$

Intuitively, rank loss occurs when candidates with low property scores have higher estimated probabilities than those with high property scores. To balance the trade-off between desired properties and similarity to original molecules, we combine the rank and cross-entropy loss as:

$$\mathcal{L} = \mathcal{L}_{\text{ce}} + \gamma \mathcal{L}_{\text{rank}},$$

where  $\gamma$  is the weight of the rank loss. Here we utilize label smoothing (Szegedy et al., 2016) to modify the target distribution of  $p_{\text{true}}$  in  $\mathcal{L}_{\text{rank}}$  to a “soft” label by assigning probability mass  $\beta$  to other tokens:

$$p_{\text{true}}(s^* | S^*, S_{<j}^*) = \begin{cases} 1 - \beta, & s^* = s_j^* \\ \frac{\beta}{N-1}, & s^* \neq s_j^* \end{cases},$$

where  $N$  is the length of the dictionary. This allows for both sequence-level coordination and token-level prediction accuracy to be taken into account, enabling the model to navigate the orientation of generated molecules effectively.

## 4. Experiments

### 4.1. Experimental Setup

**Evaluation Tasks.** We conduct experiments by comparing the proposed model, MOLGEN, with state-of-the-art approaches on three tasks. **Distribution learning** evaluates the model’s capacity to learn the data distribution and generate diverse and realistic molecules. **Targeted molecule discovery** focuses on generating novel molecules with optimized chemical properties. **Constrained molecular property optimization** aims at modifying the given molecule to improve desired properties while satisfying a similarity constraint. In addition to the three major tasks mentioned above, MOLGEN can be applied to other tasks, as detailed in Appendix A.

**Dataset.** For downstream generation tasks, the molecular data we use mainly falls into two categories: synthetic and natural product datasets. For **synthetic** datasets, we use the benchmark ZINC250k dataset (Irwin et al., 2012) containing about 250,000 drug-like molecules for the optimization task, and the ZINC-based MOSES dataset (Polykovskiy et al., 2018) containing 1,936,962 molecules for the generation task. Moreover, we collect 30,926 **natural product** compounds from the NPASS database (Zhao et al., 2022) and conduct all tasks on this dataset, detailed in Appendix B.

Table 1. Generation performance on the **Synthetic** MOSES dataset.

METHOD	VALIDITY(↑)	FRAG(↑)	SCAF(↑)	SNN(↑)	INTDIV(↑)	FCD(↓)	NOVELTY(↑)
AAE	0.9368	0.9910	0.9022	0.6081	0.8557	0.5555	0.7931
LATENTGAN	0.8966	0.9986	0.8867	0.5132	0.8565	0.2968	0.9498
CHARRNN	0.9748	0.9998	0.9242	0.6015	0.8562	0.0732	0.8419
VAE	0.9767	0.9994	0.9386	0.6257	0.8558	0.0990	0.6949
JTN-VAE	<b>1.0000</b>	0.9965	0.8964	0.5477	0.8551	0.3954	0.9143
LIMO	<b>1.0000</b>	0.9562	0.1073	0.6125	0.8544	0.1532	0.8956
CHEMFORMER-LARGE	0.9843	0.9889	0.9248	0.5622	0.8553	0.0061	0.9581
MOLGEN	<b>1.0000</b>	<b>0.9999</b>	<b>0.9999</b>	<b>0.9996</b>	<b>0.8567</b>	<b>0.0015</b>	<b>1.0000</b>

Table 2. Generation performance on the **Natural Product** dataset.

METHOD	VALIDITY(↑)	FRAG(↑)	SCAF(↑)	SNN(↑)	INTDIV(↑)	FCD(↓)	NOVELTY(↑)
AAE	0.0082	0.9687	0.2638	0.3680	0.8704	4.1089	0.9943
LATENTGAN	0.9225	0.2771	0.0884	0.5321	0.6009	45.5327	0.9949
CHARRNN	0.7351	0.8816	0.5212	0.4179	0.8756	2.2115	0.9792
VAE	0.2627	0.8840	0.4563	0.3950	0.8719	4.3175	0.9912
LIMO	<b>1.0000</b>	0.7242	0.0005	0.3416	0.7726	31.8366	0.9962
CHEMFORMER-LARGE	0.9825	0.9826	0.4126	0.5875	0.8650	0.8346	0.9947
MOLGEN	<b>1.0000</b>	<b>0.9994</b>	<b>0.8404</b>	<b>0.8148</b>	<b>0.8878</b>	<b>0.6519</b>	<b>0.9987</b>

## 4.2. Main Results

**Distribution Learning.** Distribution learning models are mainly used for building virtual libraries for computer-assisted drug discovery (van Hilten et al., 2019). Relying on a set of manually or automatically selected compounds, distribution learning models can generate a larger dataset that preserves implicit rules from the reference dataset. In this section, we adopt seven widely used metrics, detailed in Appendix E, to evaluate the ability of MOLGEN to model real molecules. We generate 10,000 molecules on the synthetic dataset following the setting in Polykovskiy et al. (2018) and 80,000 molecules on the natural product dataset.

Table 1 and 2 offer the following observations: (1) MOLGEN holds a perfect ability to produce valid molecules without additional valency check like JTN-VAE (Jin et al., 2018). Since LIMO (Eckmann et al., 2022) is also modeled based on SELFIES, the molecules it generates also have 100% validity. However, due to the complexity of internal structures and scaffolds in natural products, most models fail to produce valid molecules on the natural product dataset. The performance of Chemformer (Irwin et al., 2022) is better than others, largely because the model learns the SMILES grammar during large-scale pre-training. (2) On synthetic datasets, almost all models generate molecules with similar fragments and scaffolds to the reference molecules. However, MOLGEN excels at capturing substructure distribution in natural products. (3) MOLGEN achieves the highest SNN and lowest FCD scores, indicating that it effectively masters the statistics of the dataset in terms of biological properties and topology structure. Additionally, the good performance

Table 3. Comparison of QED and p-logP maximization methods on the synthetic ZINC dataset. As the p-logP score can increase linearly with molecule length, we divide baselines into upper and lower groups for a fair comparison. The first group of models has a limit on the output length (The maximum molecule size of ZINC250k), while the second has no limit.

METHOD	P-LOGP			QED		
	1ST	2ND	3RD	1ST	2ND	3RD
ZINC	4.52	4.30	4.23	0.948	0.948	0.948
GCPN	7.98	7.85	7.80	<b>0.948</b>	0.947	0.946
MOLDQN	11.80	11.80	11.80	<b>0.948</b>	0.943	0.943
LIMO	10.50	9.69	9.60	0.947	0.946	0.945
MOLGEN	<b>30.51</b>	<b>28.98</b>	<b>28.95</b>	<b>0.948</b>	<b>0.948</b>	<b>0.948</b>
JT-VAE	5.30	4.93	4.49	0.925	0.911	0.910
GRAPHAF	12.23	11.29	11.05	<b>0.948</b>	<b>0.948</b>	0.947
GRAPHDF	13.70	13.18	13.17	<b>0.948</b>	<b>0.948</b>	<b>0.948</b>
MARS	44.99	44.32	43.81	<b>0.948</b>	<b>0.948</b>	<b>0.948</b>
MOLGEN	<b>80.30</b>	<b>74.70</b>	<b>69.85</b>	<b>0.948</b>	<b>0.948</b>	<b>0.948</b>

of IntDiv and Novelty metrics suggests that MOLGEN is favorable for discovering new chemical structures and exploring unknown chemical space without overfitting. We provide a visual comparison of the training set and generated molecules in Appendix F.1.

**Targeted Molecule Discovery.** In this task, we aim to generate molecules with high property scores using penalized logP (p-logP) (Jin et al., 2018) and QED (Bickerton et al., 2012) as the optimization targets. P-logP refers to the logP score penalized by ring size and synthetic accessibility, while QED refers to the quantitative estimation of drug-likeness. Both scores are calculated by empirical pre-

diction models, and we utilize the script based on the official implementation of Shi et al. (2020b) to ensure comparability. Unlike the distribution learning task that only employs the basic MPT strategy, for this task, we enhance the MPT method by incorporating the self-feedback paradigm to more effectively guide the generation direction of the molecules.

In Table 3, we present the top-3 property scores of molecules generated by each model on the synthetic ZINC dataset, following the convention of previous works (Shi et al., 2020b; Eckmann et al., 2022). The first line provides a summary of the top-3 property scores of the ZINC250K dataset. For a fair comparison, we divide the baselines into two groups based on the output length. The models in the first group have a maximum output length limit, while the second group has no such restriction. As MOLGEN supports variable-length output, we compare it under these two settings.

From Table 3, we notice that MOLGEN achieves better performance than all baselines for p-logP score and obtains comparable results for QED, suggesting that the combination of multi-task molecular prefix tuning and the self-feedback paradigm effectively encourages the molecular PLM to assign higher probabilities to candidate molecules with desired properties, providing a significant advantage for optimizing molecules. However, it should be noted that the p-logP metric heavily depend on molecule length (Xie et al., 2021; Eckmann et al., 2022), and while we obtain the highest property score in the unlimited length setting for a fair comparison, large molecules such as these are unrealistic for practical drug discovery. Moreover, QED is known to have boundary effects around its maximum score of 0.948 (Zhou et al., 2019), and drugs with a QED score above 0.9 are usually very rare. Despite these limitations, the good performance of MOLGEN demonstrates its strong ability to explore the complex chemical space and generate diverse molecular graphs.

For natural products, we use shared prefixes with synthetic molecules to facilitate knowledge transfer across different domains. The results, shown in Appendix F.2 and Figure 10, demonstrate MOLGEN’s ability to generate molecules with high QED and p-logP scores. As per our reference natural product dataset, only 0.701% of molecules have a QED score greater than 0.9, with the highest score being 0.9439 (as seen in Appendix B Table 5). Thus, achieving the maximum score of 0.9478 is sufficient for practical drug discovery purposes. Additionally, MOLGEN can generate molecules with a p-logP score of 54.33, which is significantly higher than the maximum score of 17.69 in the reference set, further demonstrating MOLGEN’s strong performance in generating molecules with desired properties.

**Constrained Molecular Property Optimization.** For this task, it aims to improve the p-logP score of a given

Table 4. The average p-logP improvements of generated molecules over inputs under similarity constraint  $\delta = \{0.6, 0.4\}$ .

METHOD	IMPROVEMENT	
	$\delta = 0.6$	$\delta = 0.4$
JT-VAE	0.28±0.79	1.03±1.39
GCPN	0.79±0.63	2.49±1.30
MOLDQN	1.86±1.21	3.37±1.62
VSEQ2SEQ	2.33±1.17	3.37±1.75
VJTNN	2.33±1.24	3.55±1.67
GA	3.44±1.09	5.93±1.41
GRAPHAF	4.98±6.49	8.21±6.51
GRAPHDF	4.51±5.80	9.19±6.43
LIMO	1.80±2.00	3.60±2.30
CHEMFORMER-LARGE	2.48±0.89	3.56±1.32
MOLGEN	<b>12.08±0.82</b>	<b>12.35±1.21</b>

molecule while maintaining a similarity of at least  $\delta$  to the original molecule. Following previous works (Jin et al., 2018; Shi et al., 2020b; Luo et al., 2021; Eckmann et al., 2022), we optimize the p-logP scores of 800 molecules from the synthetic ZINC250K dataset with the lowest scores and use the Tanimoto similarity with Morgan fingerprints (Rogers & Hahn, 2010) to measure the similarity between the optimized molecules and input.

We report the mean and standard deviation of the success rate under each similarity constraint, which is the percentage of molecules that can be successfully optimized over 800 molecules. As summarized in Table 4, MOLGEN yields better results under the two similarity constraints compared to baseline models, validating its ability to search for molecules with higher property scores in the nearby chemical space. Surprisingly, MOLGEN outperforms models that rely on additional reward functions (GCPN (You et al., 2018), MoLDQN (Zhou et al., 2019), GraphAF (Shi et al., 2020b), GraphDF (Luo et al., 2021)) or property predictors (JT-VAE (Jin et al., 2018), VJTNN (Jin et al., 2019), LIMO (Eckmann et al., 2022)), further emphasizing the power of the self-feedback paradigm in MPT.

Following the same setting, we conduct experiments on the QED score for synthetic molecules and on two molecular properties for natural products using shared prefixes. Figure 11 and 12 in Appendix F.3 visually demonstrate the results of constrained optimization examples. These examples show that despite the complex molecular structure and long length of natural products, MOLGEN can improve the property score while maintaining a certain level of similarity between the input and the modified molecule. Additionally, MOLGEN is able to maintain the diversity of generated molecules while exploring the chemical space in close proximity to the input molecule.

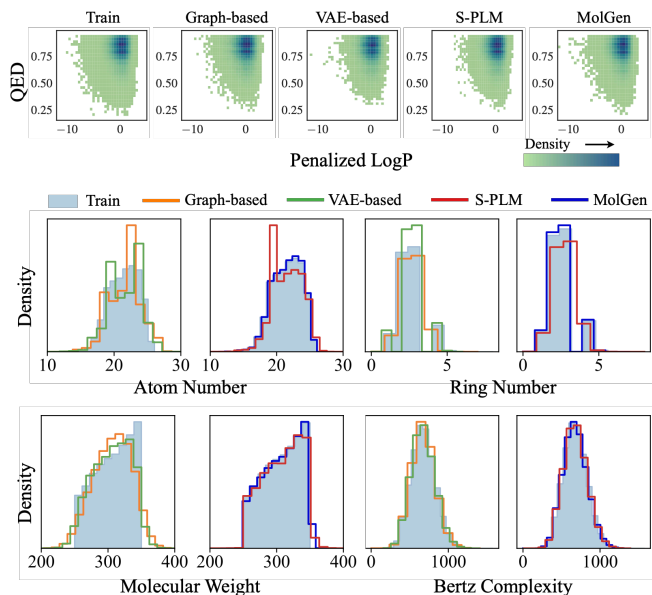


Figure 3. Comparison of molecules generated by different models on properties, atom counts, ring counts, molecular weights, and Bertz complexity (S-PLM stands for SMILES-based PLM).

#### 4.3. A Closer Look at MOLGEN

##### MOLGEN learns complex molecular distributions.

First of all, we evaluate the performance of the pre-trained MOLGEN by comparing it with the most popular deep generative Graph-based (Jin et al., 2018), VAE-based (Blaschke et al., 2018), and SMILES-based language models (Irwin et al., 2022) in terms of the distribution of properties and structures of the generated molecules. The training and generation settings of all models are the same as the distribution learning task on the synthetic MOSES dataset.

As shown in the 2D histograms of p-logP and QED scores in Figure 3, VAE-based and SMILES-based PLMs tend to produce molecules with larger p-logP and QED scores than the training data. In comparison, the Graph-based model learns the main mode of p-logP in the training data, while MOLGEN performs a bit better - similar results are observed for QED. Furthermore, in terms of molecular topology, PLMs outperform the others in perceiving atom numbers, ring numbers, and molecular weights, with MOLGEN producing a slightly closer match to the training distribution. All the models are capable of picking up on molecular Bertz complexity. Overall, PLMs, especially MOLGEN, can capture the properties and structural characteristics of the training molecules while preserving the diversity of generation.

##### MOLGEN captures molecular substructures implicitly.

In this section, we investigate the capability of PLMs to capture essential substructures when using different molecular languages (i.e., SMILES and SELFIES). To provide an

intuitive understanding, we visualize the attention weights of each token in the same molecule. Specifically, we extract and normalize the attention weights from the last self-attention layer, as illustrated in Figure 4.

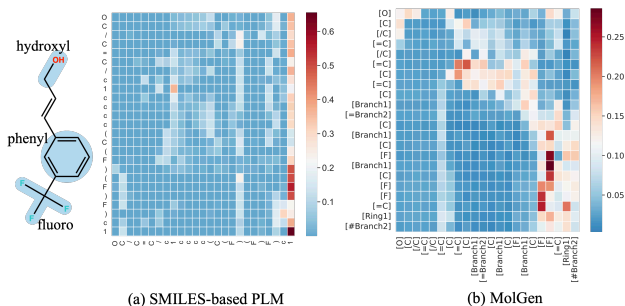


Figure 4. Visualization of learned attention maps for the same molecule by different PLM models. Note that the models we compared are of a similar parameter scale.

The attention map produced by MOLGEN shows that the *fluoro* group has higher attention weights, followed by the *phenyl* and *hydroxyl* groups. This is because the *fluoro* group has a strong ability to acquire electrons, which greatly affects the polarity of the molecule. The *phenyl* group is a frequently occurring organic functional group, while the *hydroxyl* group largely affects the interaction force between the molecule and water. However, SMILES-based PLMs may allocate more attention to symbols or numbers that are meaningless when they are independent, which may negatively impact the model’s ability to perceive frequently occurring substructures. For further illustration, additional results are presented in Figure 13 in Appendix F.4. It is clear that, by using a precise vocabulary without any meaningless tokens, MOLGEN is able to focus on tokens without distractions and capture molecular substructures implicitly.

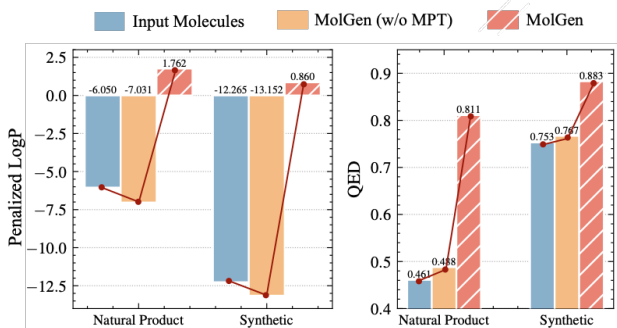


Figure 5. Property dynamics across MOLGEN stages (Figure 8 in Appendix F.2 provides a more detailed look at these changes).

##### Multi-task molecular prefix tuning facilitates property optimization.

Finally, we conduct an ablation study to investigate the impact of MPT combined with the self-feedback paradigm on the optimization of molecular properties. Starting from a batch of molecules to be optimized in



natural products and synthetic compounds, Figure 5 illustrates the changes in property scores of molecules generated by different model architectures.

Without MPT, the pre-trained model can learn similar property scores to the starting molecules. Moreover, we observe an exponential increase in scores from the first two stages to the last stage when MPT is implemented. This confirms that MPT enables MOLGEN to generate molecules with desired properties by sharing knowledge across different tasks and domains and encouraging the model to assign higher estimated probabilities to better candidate molecules.

## 5. Conclusion and Future Work

In this paper, we propose MOLGEN, a pre-trained molecular language model that utilizes the chemical language SELFIES and multi-task molecular prefix tuning to navigate knowledge sharing across diverse tasks and domains. Our in-depth study on MOLGEN demonstrates its ability to effectively identify essential molecular substructures and generate molecules with targeted properties. Interesting future directions include: 1) applying MOLGEN to other tasks such as retrosynthesis and reaction prediction (Shi et al., 2020a), 2) exploring multimodal pre-training like Edwards et al. (2022); Su et al. (2022), 3) incorporating additional sources of knowledge. We will release the pre-trained model, code and data, hoping our work has the potential to pave the way for more efficient and accurate molecular generation in various fields.

## References

- Ahn, S., Kim, J., Lee, H., and Shin, J. Guiding deep molecular optimization with genetic exploration. In *NeurIPS*, 2020.
- Atanasov, A. G., Zotchev, S. B., Dirsch, V. M., and Supuran, C. T. Natural products in drug discovery: advances and opportunities. *Nature reviews Drug discovery*, 20(3): 200–216, 2021.
- Bagal, V., Aggarwal, R., Vinod, P., and Priyakumar, U. D. Molgpt: molecular generation using a transformer-decoder model. *Journal of Chemical Information and Modeling*, 62(9):2064–2076, 2021.
- Bickerton, G. R., Paolini, G. V., Besnard, J., Muresan, S., and Hopkins, A. L. Quantifying the chemical beauty of drugs. *Nature chemistry*, 4(2):90–98, 2012.
- Blaschke, T., Olivecrona, M., Engkvist, O., Bajorath, J., and Chen, H. Application of generative autoencoder in de novo molecular design. *Molecular informatics*, 37(1-2): 1700123, 2018.
- Brown, T. B., Mann, B., Ryder, N., Subbiah, M., Kaplan, J., Dhariwal, P., Neelakantan, A., Shyam, P., Sastry, G., Askell, A., Agarwal, S., Herbert-Voss, A., Krueger, G., Henighan, T., Child, R., Ramesh, A., Ziegler, D. M., Wu, J., Winter, C., Hesse, C., Chen, M., Sigler, E., Litwin, M., Gray, S., Chess, B., Clark, J., Berner, C., McCandlish, S., Radford, A., Sutskever, I., and Amodei, D. Language models are few-shot learners. *CoRR*, abs/2005.14165, 2020. URL <https://arxiv.org/abs/2005.14165>.
- Cao, N. D. and Kipf, T. Molgan: An implicit generative model for small molecular graphs. *CoRR*, abs/1805.11973, 2018.
- Chilingaryan, G., Tamoyan, H., Tevosyan, A., Babayan, N., Khondkaryan, L., Hambardzumyan, K., Navoyan, Z., Khachatryan, H., and Aghajanyan, A. Bartsmls: Generative masked language models for molecular representations. *CoRR*, abs/2211.16349, 2022. doi: 10.48550/arXiv.2211.16349. URL <https://doi.org/10.48550/arXiv.2211.16349>.
- Du, Y., Fu, T., Sun, J., and Liu, S. Molgensurvey: A systematic survey in machine learning models for molecule design. *CoRR*, abs/2203.14500, 2022.
- Eckmann, P., Sun, K., Zhao, B., Feng, M., Gilson, M. K., and Yu, R. LIMO: latent inceptionism for targeted molecule generation. In *ICML*, volume 162 of *Proceedings of Machine Learning Research*, pp. 5777–5792. PMLR, 2022.
- Edwards, C., Lai, T., Ros, K., Honke, G., and Ji, H. Translation between molecules and natural language. *arXiv preprint arXiv:2204.11817*, 2022.
- Flam-Shepherd, D., Zhu, K., and Aspuru-Guzik, A. Language models can learn complex molecular distributions. *Nature Communications*, 13(1):1–10, 2022.
- Gómez-Bombarelli, R., Wei, J. N., Duvenaud, D., Hernández-Lobato, J. M., Sánchez-Lengeling, B., Sheberla, D., Aguilera-Iparraguirre, J., Hirzel, T. D., Adams, R. P., and Aspuru-Guzik, A. Automatic chemical design using a data-driven continuous representation of molecules. *ACS central science*, 4(2):268–276, 2018.
- Irwin, J. J., Sterling, T., Mysinger, M. M., Bolstad, E. S., and Coleman, R. G. ZINC: A free tool to discover chemistry for biology. *J. Chem. Inf. Model.*, 52(7):1757–1768, 2012.
- Irwin, R., Dimitriadis, S., He, J., and Bjerrum, E. J. Chemformer: a pre-trained transformer for computational chemistry. *Mach. Learn. Sci. Technol.*, 3(1):15022, 2022.

- Jensen, J. H. A graph-based genetic algorithm and generative model/monte carlo tree search for the exploration of chemical space. *Chemical science*, 10(12):3567–3572, 2019.
- Jin, W., Barzilay, R., and Jaakkola, T. S. Junction tree variational autoencoder for molecular graph generation. In *ICML*, volume 80 of *Proceedings of Machine Learning Research*, pp. 2328–2337. PMLR, 2018.
- Jin, W., Yang, K., Barzilay, R., and Jaakkola, T. S. Learning multimodal graph-to-graph translation for molecule optimization. In *ICLR (Poster)*. OpenReview.net, 2019.
- Jin, W., Barzilay, R., and Jaakkola, T. S. Hierarchical generation of molecular graphs using structural motifs. In *ICML*, volume 119 of *Proceedings of Machine Learning Research*, pp. 4839–4848. PMLR, 2020.
- Kenton, J. D. M.-W. C. and Toutanova, L. K. Bert: Pre-training of deep bidirectional transformers for language understanding. In *Proceedings of NAACL-HLT*, pp. 4171–4186, 2019.
- Krenn, M., Häse, F., Nigam, A., Friederich, P., and Aspuru-Guzik, A. Self-referencing embedded strings (SELFIES): A 100% robust molecular string representation. *Mach. Learn. Sci. Technol.*, 1(4):45024, 2020.
- Krenn, M., Ai, Q., Barthel, S., Carson, N., Frei, A., Frey, N. C., Friederich, P., Gaudin, T., Gayle, A. A., Jablonka, K. M., Lameiro, R. F., Lemm, D., Lo, A., Moosavi, S. M., Nápoles-Duarte, J. M., Nigam, A., Pollice, R., Rajan, K., Schatzschneider, U., Schwaller, P., Skreta, M., Smit, B., Strieth-Kalthoff, F., Sun, C., Tom, G., von Rudorff, G. F., Wang, A., White, A. D., Young, A., Yu, R., and Aspuru-Guzik, A. SELFIES and the future of molecular string representations. *Patterns*, 3(10):100588, 2022.
- Kusner, M. J., Paige, B., and Hernández-Lobato, J. M. Grammar variational autoencoder. In *ICML*, volume 70 of *Proceedings of Machine Learning Research*, pp. 1945–1954. PMLR, 2017.
- Kwon, Y., Kang, S., Choi, Y.-S., and Kim, I. Evolutionary design of molecules based on deep learning and a genetic algorithm. *Scientific reports*, 11(1):1–11, 2021.
- Lewis, M., Liu, Y., Goyal, N., Ghazvininejad, M., Mohamed, A., Levy, O., Stoyanov, V., and Zettlemoyer, L. BART: denoising sequence-to-sequence pre-training for natural language generation, translation, and comprehension. In *ACL*, pp. 7871–7880. Association for Computational Linguistics, 2020.
- Liu, Q., Allamanis, M., Brockschmidt, M., and Gaunt, A. L. Constrained graph variational autoencoders for molecule design. In *NeurIPS*, pp. 7806–7815, 2018.
- Liu, Y., Liu, P., Radev, D. R., and Neubig, G. BRIO: bringing order to abstractive summarization. In *ACL (1)*, pp. 2890–2903. Association for Computational Linguistics, 2022.
- Luo, Y., Yan, K., and Ji, S. Graphdf: A discrete flow model for molecular graph generation. In *ICML*, volume 139 of *Proceedings of Machine Learning Research*, pp. 7192–7203. PMLR, 2021.
- Ma, T., Chen, J., and Xiao, C. Constrained generation of semantically valid graphs via regularizing variational autoencoders. In *NeurIPS*, pp. 7113–7124, 2018.
- Nigam, A., Friederich, P., Krenn, M., and Aspuru-Guzik, A. Augmenting genetic algorithms with deep neural networks for exploring the chemical space. In *ICLR*. OpenReview.net, 2020.
- Ouyang, L., Wu, J., Jiang, X., Almeida, D., Wainwright, C., Mishkin, P., Zhang, C., Agarwal, S., Slama, K., Gray, A., et al. Training language models to follow instructions with human feedback. In *Advances in Neural Information Processing Systems*, 2022.
- Pan, J. Large language model for molecular chemistry. *Nature Computational Science*, pp. 1–1, 2023.
- Polishchuk, P. G., Madzhidov, T. I., and Varnek, A. Estimation of the size of drug-like chemical space based on GDB-17 data. *J. Comput. Aided Mol. Des.*, 27(8): 675–679, 2013.
- Polykovskiy, D., Zhebrak, A., Sánchez-Lengeling, B., Golovanov, S., Tatanov, O., Belyaev, S., Kurbanov, R., Artamonov, A., Aladinskiy, V., Veselov, M., Kadurin, A., Nikolenko, S. I., Aspuru-Guzik, A., and Zhavoronkov, A. Molecular sets (MOSES): A benchmarking platform for molecular generation models. *CoRR*, abs/1811.12823, 2018.
- Popova, M., Isayev, O., and Tropsha, A. Deep reinforcement learning for de novo drug design. *Science advances*, 4(7): eaap7885, 2018.
- Popova, M., Shvets, M., Oliva, J., and Isayev, O. Molecular-rnn: Generating realistic molecular graphs with optimized properties. *CoRR*, abs/1905.13372, 2019.
- Rogers, D. and Hahn, M. Extended-connectivity fingerprints. *J. Chem. Inf. Model.*, 50(5):742–754, 2010.
- Ross, J., Belgodere, B., Chenthamarakshan, V., Padhi, I., Mroueh, Y., and Das, P. Large-scale chemical language representations capture molecular structure and properties. *Nature Machine Intelligence*, 4(12):1256–1264, 2022.

- Segler, M. H., Kogej, T., Tyrchan, C., and Waller, M. P. Generating focused molecule libraries for drug discovery with recurrent neural networks. *ACS central science*, 4(1):120–131, 2018.
- Shi, C., Xu, M., Guo, H., Zhang, M., and Tang, J. A graph to graphs framework for retrosynthesis prediction. In *Proceedings of the 37th International Conference on Machine Learning, ICML 2020, 13-18 July 2020, Virtual Event*, volume 119 of *Proceedings of Machine Learning Research*, pp. 8818–8827. PMLR, 2020a. URL <http://proceedings.mlr.press/v119/shi20d.html>.
- Shi, C., Xu, M., Zhu, Z., Zhang, W., Zhang, M., and Tang, J. Graphaf: a flow-based autoregressive model for molecular graph generation. In *ICLR*. OpenReview.net, 2020b.
- Simonovsky, M. and Komodakis, N. Graphvae: Towards generation of small graphs using variational autoencoders. In *ICANN (1)*, volume 11139 of *Lecture Notes in Computer Science*, pp. 412–422. Springer, 2018.
- Sterling, T. and Irwin, J. J. ZINC 15 - ligand discovery for everyone. *J. Chem. Inf. Model.*, 55(11):2324–2337, 2015.
- Su, B., Du, D., Yang, Z., Zhou, Y., Li, J., Rao, A., Sun, H., Lu, Z., and Wen, J.-R. A molecular multimodal foundation model associating molecule graphs with natural language. *arXiv preprint arXiv:2209.05481*, 2022.
- Sun, M., Xing, J., Meng, H., Wang, H., Chen, B., and Zhou, J. Molsearch: Search-based multi-objective molecular generation and property optimization. In *KDD*, pp. 4724–4732. ACM, 2022.
- Szegedy, C., Vanhoucke, V., Ioffe, S., Shlens, J., and Wojna, Z. Rethinking the inception architecture for computer vision. In *CVPR*, pp. 2818–2826. IEEE Computer Society, 2016.
- van Hilten, N., Chevillard, F., and Kolb, P. Virtual compound libraries in computer-assisted drug discovery. *J. Chem. Inf. Model.*, 59(2):644–651, 2019.
- Vaswani, A., Shazeer, N., Parmar, N., Uszkoreit, J., Jones, L., Gomez, A. N., Kaiser, L., and Polosukhin, I. Attention is all you need. In Guyon, I., von Luxburg, U., Bengio, S., Wallach, H. M., Fergus, R., Vishwanathan, S. V. N., and Garnett, R. (eds.), *Advances in Neural Information Processing Systems 30: Annual Conference on Neural Information Processing Systems 2017, December 4-9, 2017, Long Beach, CA, USA*, pp. 5998–6008, 2017. URL <https://proceedings.neurips.cc/paper/2017/hash/3f5ee243547dee91fbd053c1c4a845aa-Abstract.html>.
- Wang, M., Wang, Z., Sun, H., Wang, J., Shen, C., Weng, G., Chai, X., Li, H., Cao, D., and Hou, T. Deep learning approaches for de novo drug design: An overview. *Current Opinion in Structural Biology*, 72:135–144, 2022a.
- Wang, Z., Nie, W., Qiao, Z., Xiao, C., Baraniuk, R. G., and Anandkumar, A. Retrieval-based controllable molecule generation. *CoRR*, abs/2208.11126, 2022b.
- Weininger, D. Smiles, a chemical language and information system. 1. introduction to methodology and encoding rules. *J. Chem. Inf. Comput. Sci.*, 28(1):31–36, 1988.
- Winter, R., Montanari, F., Steffen, A., Briem, H., Noé, F., and Clevert, D.-A. Efficient multi-objective molecular optimization in a continuous latent space. *Chemical science*, 10(34):8016–8024, 2019.
- Xie, Y., Shi, C., Zhou, H., Yang, Y., Zhang, W., Yu, Y., and Li, L. MARS: markov molecular sampling for multi-objective drug discovery. In *ICLR*. OpenReview.net, 2021.
- You, J., Liu, B., Ying, Z., Pande, V. S., and Leskovec, J. Graph convolutional policy network for goal-directed molecular graph generation. In *NeurIPS*, pp. 6412–6422, 2018.
- Zang, C. and Wang, F. Moflow: An invertible flow model for generating molecular graphs. In *KDD*, pp. 617–626. ACM, 2020.
- Zhao, H., Yang, Y., Wang, S., Yang, X., Zhou, K., Xu, C., Zhang, X., Fan, J., Hou, D., Li, X., et al. Npass database update 2023: quantitative natural product activity and species source database for biomedical research. *Nucleic Acids Research*, 2022.
- Zhou, Z., Kearnes, S., Li, L., Zare, R. N., and Riley, P. Optimization of molecules via deep reinforcement learning. *Scientific reports*, 9(1):1–10, 2019.

## A. Availability of MOLGEN

We will release MOLGEN on **Hugging Face** to support the wider scientific community soon. Note that in addition to the three major tasks discussed in this paper, MOLGEN can also be simply applied to other tasks such as reaction prediction and retrosynthetic analysis. However, due to limitations in computing resources, we have only conducted experiments on the three generation tasks in this study. We leave the other tasks as our future work.

## B. Data Information

In this section, we present additional information about the dataset used in our study. For the natural product dataset, we sourced 30,926 compounds from the Natural Product Activity & Species Source Database (NPASS)<sup>3</sup> (Zhao et al., 2022). From this, we randomly selected 30,126 molecules for training and 800 molecules for testing and used the same sets for all downstream molecule generation tasks.

The statistics of our datasets are shown in Table 5. It can be observed that the natural product dataset has a distinct distribution compared to the synthetic dataset, with a wider range of p-logP scores and lower QED scores. This highlights the added complexity of optimizing the properties of natural products.

Table 5. Data statistics.

DATASET	LENGTH			PENALIZED LOGP			QED		
	MIN	MAX	MEAN	MIN	MAX	MEAN	MIN	MAX	MEAN
MOSES	13	55	35	-10.241	3.329	-0.027	0.191	0.948	0.807
ZINC250K	8	72	37	-22.189	5.073	-0.622	0.117	0.948	0.732
NATURAL PRODUCT	2	436	55	-51.083	17.691	-2.186	0.005	0.944	0.438

## C. Comparison with SMILES-based PLM

In this section, we compare the differences between two molecular language models, Chemformer (Irwin et al., 2022) and MOLGEN. For fairness, we select the large version of Chemformer for comparison in our paper, as it has a similar architecture to MOLGEN. We utilize the same number of pre-training data of 100M from the ZINC-15 dataset (Sterling & Irwin, 2015). MOLGEN utilizes a smaller and more specific vocabulary size of 185, while Chemformer uses a vocabulary size of 523. This allows MOLGEN to more effectively capture important molecular substructure information.

## D. Compared Baselines

We illustrate the baselines we compare within our experiments. We reproduce these baselines using their open-source codes and under the same experimental settings. The baselines include:

- JT-VAE (Jin et al., 2018), a VAE-based generative model which generates a scaffold junction tree and assembles nodes in the tree into a molecular graph.
- GCPN (You et al., 2018), a reinforcement learning-based method that can construct a molecule by optimizing a reward composed of adversarial loss and molecular property objectives.
- MolGQN (Zhou et al., 2019), a reinforcement learning-based method that utilizes double Q-learning and chemical domain knowledge.
- MARS (Xie et al., 2021), a sampling approach based on Markov chain Monte Carlo using an adaptive fragment-editing proposal distribution with GNN.
- GraphAF (Shi et al., 2020b), an autoregressive flow model that generates molecular graphs by adding edges and nodes sequentially.
- GraphDF (Luo et al., 2021), a normalizing flow model using a discrete latent variable model and is fine-tuned with reinforcement learning.

<sup>3</sup><https://bidd.group/NPASS/>



- LIMO (Eckmann et al., 2022), a VAE-based model that leverages a variational autoencoder-generated latent space.
- Chemformer (Irwin et al., 2022), a pre-trained molecular language model that conducts on SMILES representations.

## E. Experiment Metrics and Details

In this section, we describe the evaluation metrics, training procedures, and hyperparameters used for each task and dataset in our experiments. MOLGEN is implemented using Pytorch and trained on 6 Nvidia V100 GPUs. For pre-training, we use the LAMB optimizer with a linear warm-up of the learning rate for the first 180,000 gradient updates, followed by a linear decay for the remaining training steps. The pre-training process consisted of 600 million steps with a batch size of 256 molecules per GPU. We present the specific experimental settings and parameters in Table 6.

Table 6. Hyper-parameter settings.

HYPER-PARAMETERS	VALUE
MAXIMUM SEQUENCE LENGTH	{55, 148, 436}
LEARNING RATE	{1E-5, 3E-5, 1E-4}
BATCH SIZE	{8, 32, 64, 200, 256}
WEIGHT OF RANK LOSS $\gamma$	{1, 3, 5}
PREFIX LENGTH	5

**Multi-task Molecular Prefix Tuning** To efficiently share parameters and knowledge, we first pre-train a prefix on all tasks and datasets. Next, we initialize the prefix for each task with this pre-trained prefix and then optimize it for the specific task. It is important to note that during our experiments, we empirically find that using Multi-task molecular Prefix Tuning (MPT) across various molecular tasks and data sources **does not result in negative transfer**. Therefore, we implement it on all tasks and datasets to achieve the best performance.

**Distribution Learning** We outline the metrics used to evaluate the performance of the generative models in our experiments, including:

- *Validity* measures the proportion of generated molecules conforming to valence rules.
- *Fragment similarity (Frag)*, which compares the distribution of BRICS fragments in the generated and reference sets. For example, the Frag metric will be large if the molecules in both sets have similar fragments. Conversely, if some fragments are over- or under-represented (or never present) in the generated set, the metric will be low.
- *Scaffold similarity (Scaff)*, which compares the frequencies of Bemis–Murcko scaffolds (contains all molecule’s linker fragments connecting rings and ring structures) in the generated and reference sets. That is, if the model rarely produces a specific chemotype from a reference set, the metric will be low.
- *Similarity to the nearest neighbor (SNN)*, which measures the average Tanimoto similarity between a molecule from the generated set and its nearest neighbor molecule in the reference dataset. If generated molecules are far from the manifold of the reference set, then the similarity to the nearest neighbor will be low.
- *Internal diversity (IntDiv)*, which assesses the chemical diversity of generated molecules by calculating the average Tanimoto coefficient within the generated set.
- *Fréchet ChemNet Distance (FCD)*, which considers chemically and biologically relevant information about molecules. It can detect if generated molecules have similar biological and chemical properties as real molecules.
- *Novelty*, which measures the percentage of the generated molecules that do not appear in the training set and assesses the ability to explore unknown chemical space.

To obtain the results presented in Table 1 and 2, MOLGEN is trained using the AdamW optimizer with a batch size of 200 for the MOSES dataset and 32 for the natural product dataset on 6 Nvidia V100 GPUs for 100 epochs. A linear warm-up of 20000 steps was also employed.

**Targeted Molecule Discovery / Constrained Molecular Property Optimization** For both targeted molecule discovery and constrained property optimization, we first use the pre-trained MOLGEN to generate 30 candidates for each data sample in synthetic compounds and 8 candidates for natural products and then train the model on 6 Nvidia V100 GPUs for 100 epochs. The batch size is set to 6 for the synthetic dataset and 6 for the natural product dataset. We use AdamW as the optimizer, with a linear warm-up of 20000 steps.

## F. Additional Visualization of Molecules Generated in Generation Tasks

### F.1. Distribution Learning.

In this section, we provide additional visualizations of the molecules generated by MOLGEN in the distribution learning task. Figures 6 and 7 show a comparison of molecules from the training set and those generated by MOLGEN for both synthetic and natural product datasets. The visualizations demonstrate that MOLGEN effectively captures the structural characteristics of molecules from different domains, despite their distinct differences in structure.

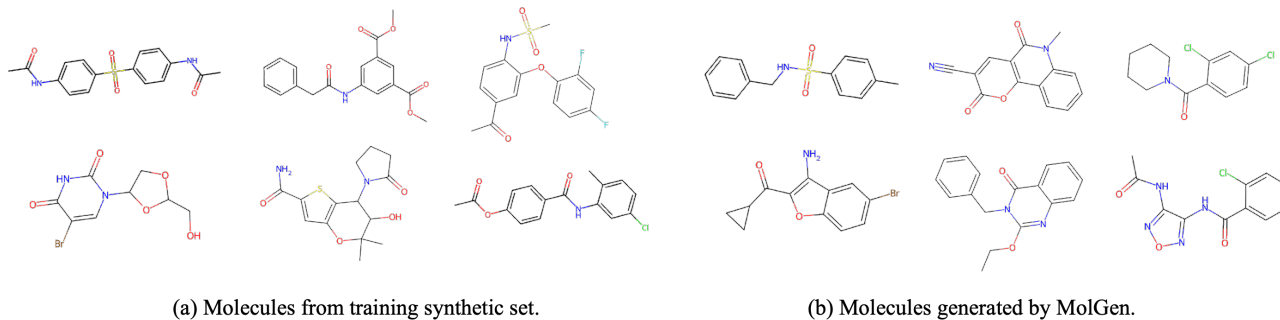


Figure 6. Visualizations of training and generated molecules of **Synthetic** compounds.

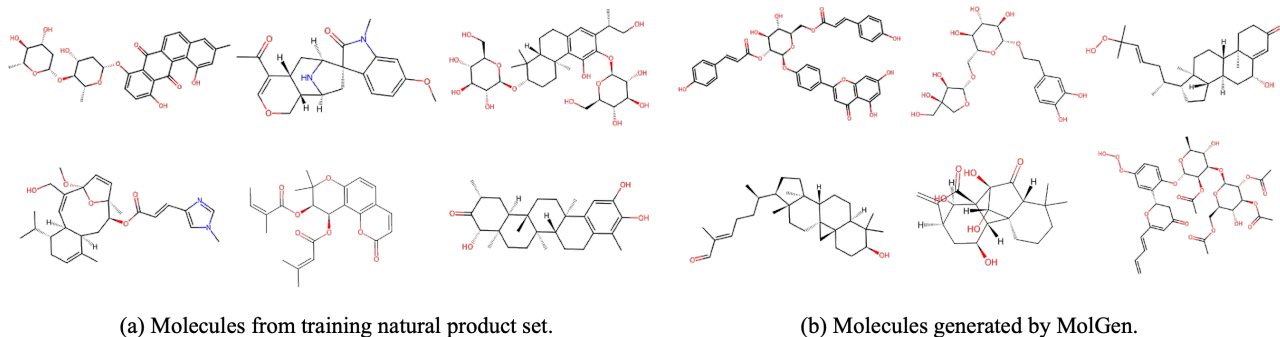


Figure 7. Visualizations of training and generated molecules of **Natural Products**.

## F.2. Targeted Molecule Discovery.

In this section, we provide additional visualizations to further support our claims in the main text. To show in more detail the molecular property changes in Figure 5, we visualize the distribution dynamics of p-logP and QED scores in Figure 8. This helps to confirm that our pre-trained MOLGEN model is able to effectively learn the property distribution of molecules and that the use of MPT improves the scores of generated molecules, moving them closer to the desired properties.

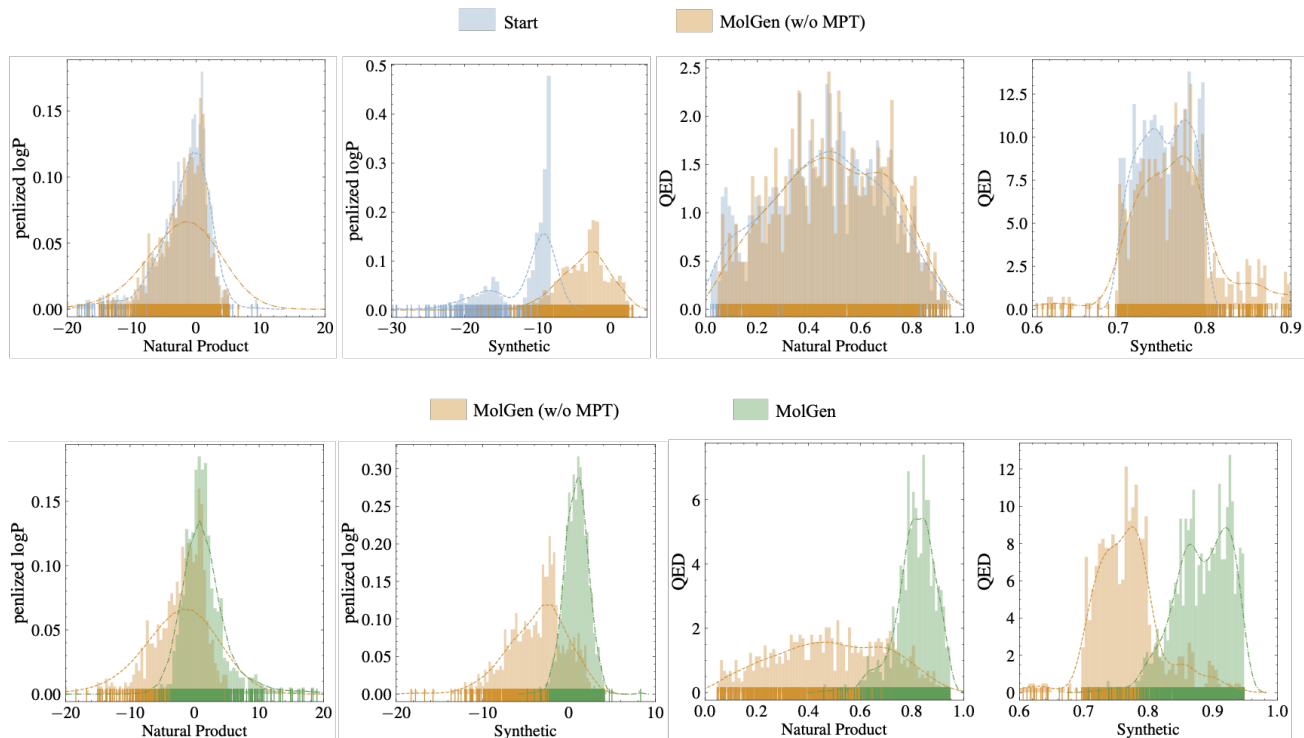


Figure 8. Property distribution dynamics across MOLGEN stages.

Moreover, the generated molecules that achieve the largest scores on both data sources are shown in Figure 9 and 10. We can conclude that although ultra-long carbon chains are typical structures of high p-logP molecules, MOLGEN can still maintain high scores without losing diversity. Besides, MOLGEN is capable of generating molecules with high QED scores while maintaining the structural properties of different domains.

## F.3. Constrained Molecular Property Optimization.

We further illustrate several constrained optimization examples of both QED and p-logP in Figure 11 and 12. These examples further demonstrate MOLGEN’s ability to optimize molecules while preserving their general structure. Furthermore, MOLGEN can also achieve good performance on more difficult natural product generation tasks, which illustrates its ability to explore broader chemical space.

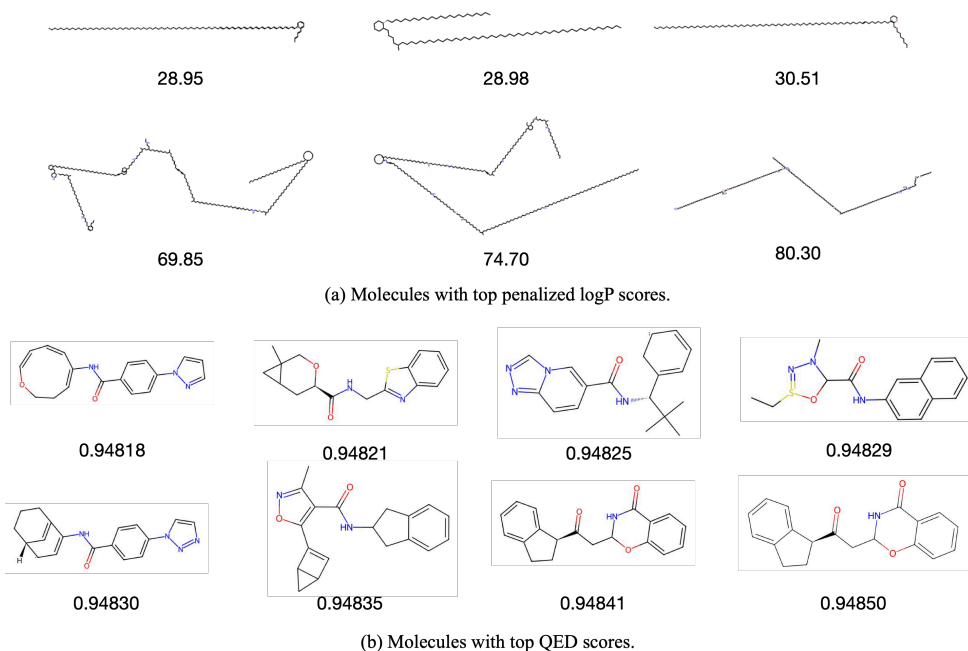


Figure 9. Molecule samples with high p-logP and QED score generated by MOLGEN from **Synthetic** compounds.

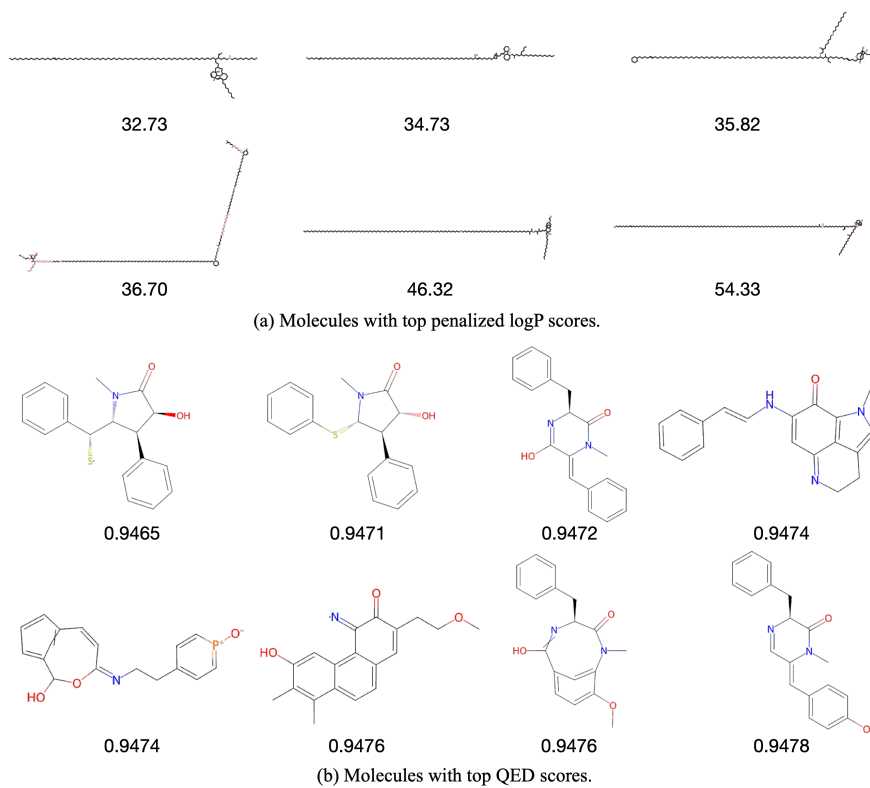


Figure 10. Molecule samples with high p-logP and QED score generated by MOLGEN from **Natural Products**.



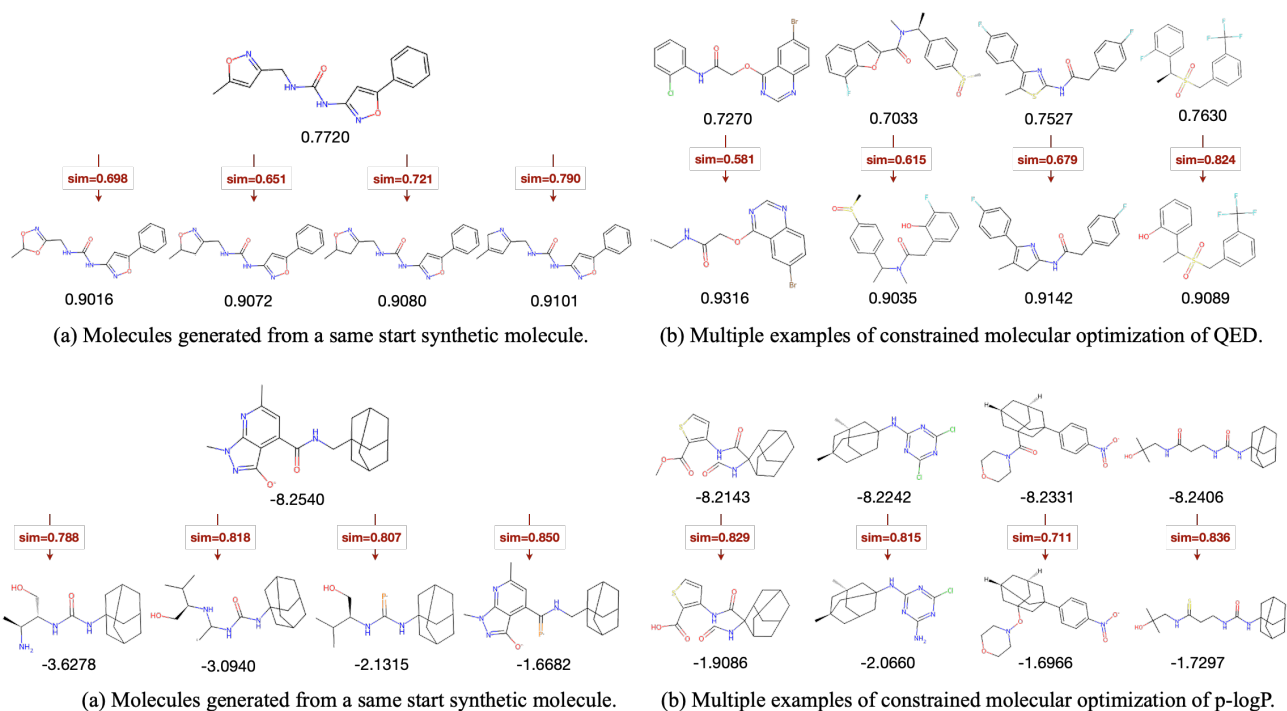


Figure 11. Illustrations of **Synthetic** molecules in constrained optimization of QED and p-logP.

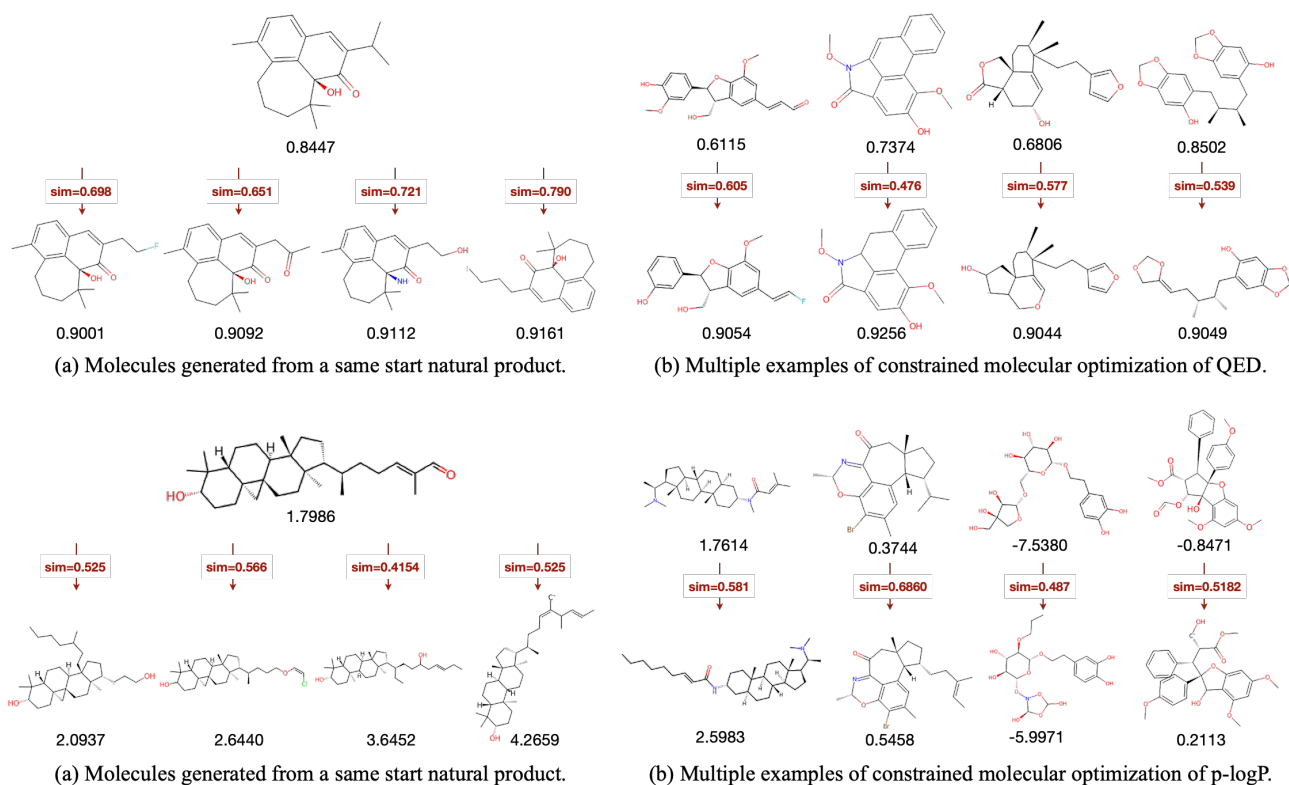


Figure 12. Illustrations of **Natural Products** in constrained optimization of QED and p-logP.

Lastly, we evaluate the representation capabilities of different PLMs by visualizing the attention weights of each token in the same molecule, using the same setting as shown in Figure 4.